Reaction Kinetics, Mechanisms and Catalysis (2019) 126:737–759
https://doi.org/10.1007/s11144-018-1502-1

Hydrodeoxygenation of phenolic model compounds over zirconia supported Ir and Ni-catalysts

Moldir Alda-Onggar[1] · Päivi Mäki-Arvela[1] · Atte Aho[1] · Irina L. Simakova[2] · Dmitry Yu. Murzin[1]

Received: 10 September 2018 / Accepted: 15 November 2018 / Published online: 22 November 2018

Abstract

The hydrodeoxygenation (HDO) of three different phenolic model compounds, isoeugenol, guaiacol and vanillin was investigated using Ir/ZrO_2 and Ni/ZrO_2 as heterogeneous catalysts. The catalysts were prepared by incipient wetness impregnation and characterized by transmission electron microscopy, nitrogen adsorption, FTIR pyridine adsorption–desorption. The organic material in the spent catalysts was analyzed by organic elemental analysis and thermogravimetry. The results revealed that in guaiacol HDO at 250 °C under 30 bar total pressure the main product was cyclohexanol with 36% yield over Ni/ZrO_2 while the total deoxygenation forming cyclohexane was limited to 2%. Ir/ZrO_2 exhibited higher HDO activity compared to Ni/ZrO_2 giving 14% yield of cyclohexane. Extensive formation of methane and ethane was also observed in guaiacol HDO. Hydrodeoxygenation of isoeugenol over Ir/ZrO_2 resulted in maximally 33% yield of propylcyclohexane due to a low liquid phase mass balance. The main products in vanillin HDO at 100 °C in water was vanillyl alcohol.

Keywords Hydrodeoxygenation · Phenolic compounds · Heterogeneous catalyst · Nickel · Iridium

Electronic supplementary material The online version of this article (https://doi.org/10.1007/s11144-018-1502-1) contains supplementary material, which is available to authorized users.

✉ Päivi Mäki-Arvela
pmakiarv@abo.fi

[1] Johan Gadolin Process Chemistry Centre, Åbo Akademi University, Turku, Finland

[2] Boreskov Institute of Catalysis, Novosibirsk, Russia

Introduction

The hydrodeoxygenation of lignin derived bio-oils is currently an important research area due to depleting fossil fuel resources. Bio-oils as such are not suitable as fuels due to high acidity, oxygen content and instability [1]. There exist already some publications from the HDO of bio-oils [2, 3], but due to complicated analytics, several model compounds have been very often used including guaiacol [4], vanillin [5, 6], isoeugenol [7], anisole [8], phenol [9, 10] and cresol [11]. The use of model compounds also facilitates easier elucidation of the reaction mechanism [9]. Several attempts has also been made to elucidate the potential industrial application of the HDO of phenolic compounds, e.g. performing HDO of their mixtures in the absence of any other solvents [12]. One example of this type of experiments was HDO of the vanillin–guaiacol mixture at 200 °C under 30 bar hydrogen [12]. Only vanillin gave large amounts of partially deoxygenated product, *p*-creosol, under these conditions, whereas guaiacol did not produce any deoxygenated products. This result showed clearly some challenges in up-scaling HDO since different phenolic compounds are adsorbed on the surface with different strength depending on their structure and a number of oxygen atoms.

Several catalysts have been applied, e.g. metals (Pt, Pt–Sn, Pd, Ru) supported on carbon [5], zeolites [7], carbides [6] and oxides [8]. Bifunctional catalysts, containing both metal and acidic functionality have also been used [7]. The aim in this work was to make a comparative HDO study of three phenolic compounds, namely vanillin, guaiacol and isoeugenol (Fig. 1) using zirconia supported metals, nickel and iridium as catalysts. It is known that zirconia based catalysts exhibit oxophilic sites promoting adsorption of oxygenated compounds. For example Ni/ZrO_2 was successfully used as a catalyst in continuous hydrodeoxygenation of m-cresol in dodecane under 40 bar total pressure in hydrogen at 340 °C giving as the main products deoxygenated methylcyclohexane and methylcyclohexenes [13]. On the other hand, nearly twofold more oxygenates were formed over Ni/SiO_2 under the same conditions showing the importance of the support.

The HDO of guaiacol, eugenol and vanillin has been already demonstrated over metal supported ZrO_2 (Table 1) [4, 14, 15]. HDO of guaiacol was reported to be the most successful over $Ni/SiO_2–ZrO_2$ giving 97% yield of methylcyclohexane at 300 °C and 50 bar catalyst in 8 h [15]. The second best catalyst was 10 wt% Ni/ZrO_2 catalyst giving 75% selectivity of cyclohexane at 44% of conversion of guaiacol (entries 2 and 3). On the other hand, 5 wt% Ni/ZrO_2 resulted in 30% yield of cyclohexane at complete guaiacol conversion (entry 3). Furthermore, the calcined and reduced 5 wt% Ni/ZrO_2 resulted in higher cyclohexane selectivity (30%) than the non-treated catalyst directly used giving only 1% of cyclohexane. This result indicates that calcination is very important to activate the catalyst and enhance hydrodeoxygenation. The HDO activities of 3 wt% Rh/ZrO_2 and 5 wt% Ru/ZrO_2 were not very high with these catalysts producing mainly hydrogenated products such as 2-methoxycyclohexanol (89% and 36%) and cyclohexanol

(5 and 36%) [16]. Bimetallic catalysts supported on zirconium oxide exhibited high yields of alcohols but no deoxygenated compounds (entry 7). Summarizing guaiacol HDO, it can be stated that in order to achieve high selectivity to hydrodeoxygenated compounds, a high hydrogen pressure and a relatively high temperature are required, especially with Ni/ZrO_2 [15]. Eugenol hydrodeoxygenation was demonstrated over Co/ZrO_2 at 200 °C under 10 bar hydrogen in dodecane as a solvent [14] giving propylcyclohexanol as the main product with 57% yield at complete conversion. Co/ZrO_2 exhibited strong acidity determined by ammonia TPD.

As a comparison to guaiacol HDO over Ni/SiO_2–ZrO_2, vanillin was not converted completely (83%) in 8 h at 300 °C and 50 bar in a mixture of cresol, phenol, eugenol, trans-anethole and vanillin [4]. The main product was methylcyclohexane with 65% selectivity at 83% conversion [4], showing that vanillin is more difficult to deoxygenate in comparison to other phenolic compounds present in the mixture for which complete conversion was obtained. Selectivity to propylcyclohexane was 98% at 300 °C under 50 bar in 8 h [4] indicating that zirconia support is beneficial in HDO which can be related to both acidic and basic sites available in zirconia.

Typically, vanillin HDO has been performed in water [5, 6], and as a comparison to our previous vanillin HDO over metal supported on carbon [5], water was also used in this work as a solvent in vanillin HDO. In the previous study with Pd/C at 100 °C under 30 bar total pressure in hydrogen [5] the main product was *p*-creosol.

The aim in this work was to investigate the potential of oxophilic ZrO_2 to be used as a support for metal in HDO of phenolic compounds. According to our knowledge Ni/ZrO_2 and Ir/ZrO_2 have not been used as catalysts in vanillin HDO in water and in isoeugenol HDO. Nickel is a cheap transition metal, whereas Ir in comparison with Pt exhibits hydrogenolysis activity [20] and a homogeneous Ir catalyst was successfully used in the hydrodeoxygenation of 2,5-hexadione [21]. Thus it was decided to use Ir/ZrO_2 as a catalyst in this work. One of the main aims was also to study the liquid phase mass balance closure, since in several papers [14, 22, 23], in addition to reactant conversion the product selectivity has been defined as the ratio between the products formed not reflecting the carbon balance in liquid phase. The mass balance closure, however, can only be found in a very few papers [7, 24–27]. The experiments in this study were performed using a low initial concentration of reactants, which, however, facilitated to directly compare the performance of ZrO_2 supported catalysts (Pt/C, Pd/C, Pt/H-Beta-300, Ir–Re/Al_2O_3, with other ones applied under the same conditions [5, 7, 12, 26].

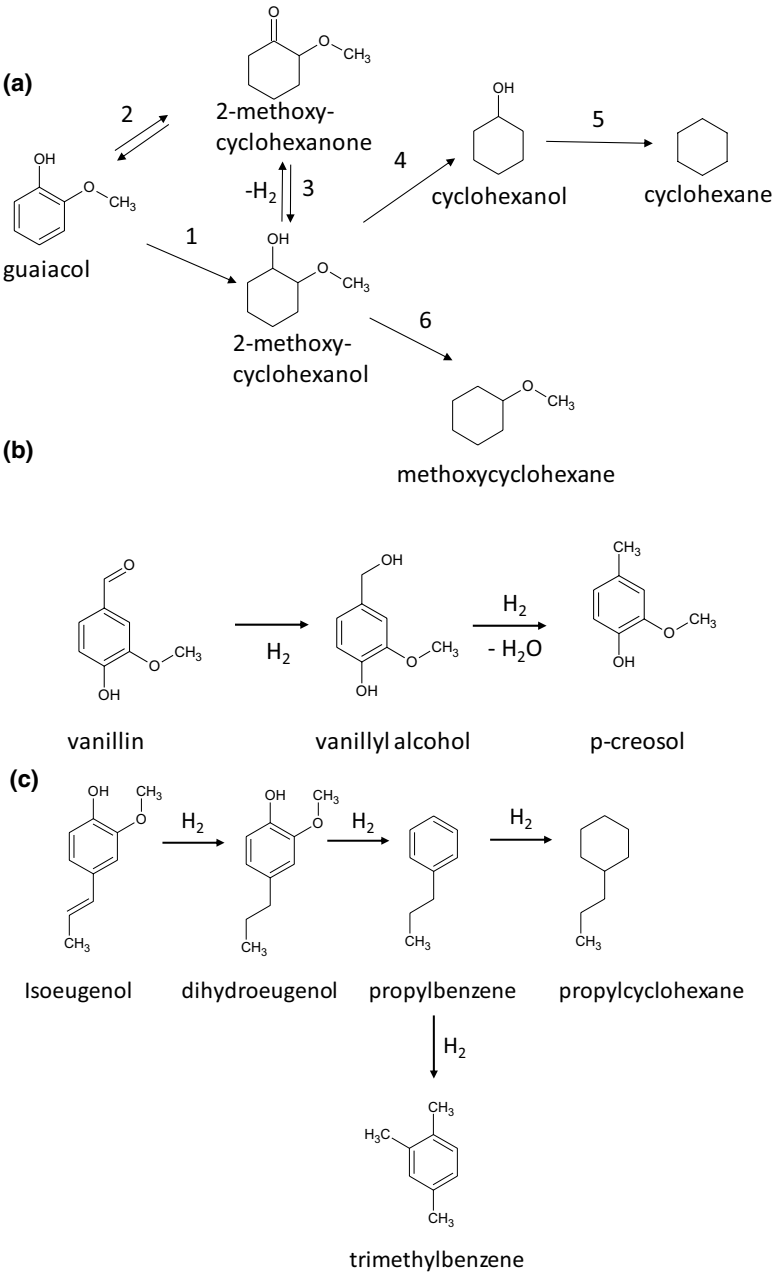

Fig. 1 Reaction schemes for HDO of **a** guaiacol, **b** vanillin and **c** isoeugenol. Notation: the trivial names for the compounds in vanillin HDO are vanillin (4-hydroxy-3-methoxybenzaldehyde), vanillyl alcohol (4-hydroxy-3-methoxybenzyl alcohol) and *p*-creosol (2-methoxy-4-methylphenol)

Table 1 Results of guaiacol HDO at different operational conditions using zirconium oxide supported catalysts

Entry	Catalyst	Solvent	Conversion of guaiacol (%)	Operational conditions (reaction duration, temperature, pressure)	Main products (yield %)	References
1	$Ni/SiO_2–ZrO_2$	Octane	100	8 h, 300 °C and 50 bar	Cyclohexane 97%	[14]
2	5 wt% Ni/ZrO_2-DR	1-Octanol	100	250 °C and 100 bar	Cyclohexanol (30%)	[16]
3	5 wt% Ni/ZrO_2-CR	1-Octanol	100	250 °C and 100 bar	Cyclohexanol (50%)	
4	10 wt% Ni/ZrO_2	Dodecane	44	8 h, 300 °C and 50 bar	Cyclohexane (75%)	[14]
5	3 wt% Rh/ZrO_2	*n*-Decane	99	1 h, 250 °C and 40 bar	2-Methoxycyclohexanol (89%)	[15]
6	5 wt% Ru/ZrO_2	Water	99	4 h, 170 °C and 40 bar	Cyclohexanol (58%)	[17]
7	$RhPt/ZrO_2$	*n*-Hexadecane	≈100	100 °C, 80 bar	1-Methyl-1,2-cyclohexanediol, cyclohexanol	[18]

DR directly reduced, *CR*-calcined and reduced

Experimental

Preparation of catalysts

All starting materials were reagent grade chemicals such as $Ni(NO_3)_2{\cdot}6H_2O$ ($\geq$98.0%, GOST 405570, Souzchimprom, Novosibirsk), $IrCl_3$ hydrate (TU 2625-067-00196533-2002 OAO "V.N. Gulidov Krasnoyarsk factory of nonferrous metals, Krasnoyarsk)", zirconia (Acros Organics, $S_{BET} = 106\ m^2/g$).

Zirconia was precalcined in air at 500 °C for 2 h before catalysts preparation. 3 wt% Ir/ZrO_2 was prepared by incipient wetness impregnation with an aqueous solution of $IrCl_3$ hydrate, sequentially dried at 110 °C for 17 h and reduced by molecular hydrogen from room temperature up to 400 °C with a ramp rate of 2 °C/min, thereafter holding in hydrogen during 3 h to remove the excess of chloride.

10 wt% Ni/ZrO_2 was prepared by incipient wetness impregnation with an aqueous solution of a nickel nitrate precursor, sequentially dried at 110 °C for 17 h, calcined in air at 540 °C for 2 h and reduced by molecular hydrogen from room temperature up to 450 °C with a ramp rate of 2 °C/min, thereafter holding in hydrogen during 3 h. The reduction temperature, 450 °C should be enough to reduce NiO [28].

Catalyst characterization methods

Nitrogen adsorption

Specific surface area of the catalysts were determined using nitrogen adsorption at 77 K using Carlo Erba Sorptomatic 1900. BET program was applied to identify the specific surface area and pore volume of the alumina supported catalysts. The investigated catalysts were heated at 150 °C and outgassed at a pressure lower than 8 mbar for 3 h.

Acidity measurement with pyridine adsorption desorption by FTIR

FTIR spectroscopy ATI Mattson with pyridine (Sigma-Aldrich, $\geq$99.5%, a.r.) adsorption desorption was used to determine the amount and strength of Brønsted and Lewis acid sites. Initially, a sample of the catalyst was pressed into a thin pellet with the weight in the range between 10 and 20 mg. The prepared pellet was placed in the cell of the spectrometer for 1 h outgassing in vacuum at 450 °C. Afterwards, the sample was cooled down to the set temperature of 100 °C, followed by adsorption of pyridine on the pellet surface for 30 min and then recording the scanned spectra. Subsequently, to obtain the acidity strength distribution such as presence of weak, medium and strong Brønsted and Lewis acid sites, the thermal desorption of pyridine was performed at 250 °C, 350 °C and 450 °C. The spectral bands integrated at 1455 cm^{-1} and 1545 cm^{-1} provided the data on the Brønsted and Lewis acid sites concentrations using extinction coefficients of Emeis [29].

Scanning electron microscopy and X-ray microanalysis (SEM–EDX)

The scanning electron microscopy coupled with energy dispersive X-ray analyzer was utilized to obtain information on the morphology and elemental analysis of the fresh and spent catalysts. Zeiss Leo Gemini 1530 microscope combined with secondary electron and backscattered electron detectors was applied for this purpose. Acceleration voltage of 15 kV was used for X-ray analyzer. In order to perform analysis, the catalyst was placed as a thin layer on top of the carbon coating to enhance the conductivity allowing high quality of magnified images.

Transmission electron microscopy (TEM)

Transmission electron microscopy was utilized to study the morphology and metal particle size. The equipment used for analysis was JEM-1400Plus (by JEOL Ltd. Japan) of 120 kV maximal acceleration voltage. The interpretation of TEM images and determination of the particles sizes of the fresh and spent catalysts were done using ImageJ program.

Thermogravimetric analysis (TGA)

Thermogravimetric characterization of the fresh and spent catalysts was carried out using SDT Q600 (V20.9 Build 20) device under nitrogen. Around 7 mg of the catalyst was placed on an aluminum oxide (Al_2O_3) sample pan as well as an empty pan on the reference and heated from room temperature to 1000 °C (temperature ramp—10 °C/min). The volumetric gas flow rate during analysis was 100 ml/min. The organic compounds and coke adsorbed on the catalyst surface have been calculated from the difference between the spent and fresh catalyst weight losses in the temperature range of 100–1000 °C, i.e. not considering the amount of water desorbed.

Catalytic experiments

HDO of isoeugenol and guaiacol was performed in an autoclave with the initial concentrations of 0.012 mol/l and 0.016 mol/l, respectively using 50 ml of dodecane (Alfa Aesar, $\geq 99\%$) as a solvent. In a typical experiment 50 mg of the prereduced catalyst was put into the reactor together with the reactant. 1 day prior to HDO of isoeugenol and guaiacol, the fresh catalysts were reduced with hydrogen (AGA, 99.999%). First, 50 mg of the catalyst was flushed with argon flow for 10 min and then with hydrogen for 10 min. The program was set to heat up from room temperature to 350 °C with 10 °C/min and keep at 350 °C for 3 h under hydrogen flow. Afterwards, as the program was completed and temperature decreased to 100 °C, the catalyst was flushed with argon (AGA, 99.999%) for 10 min and 10 ml of the solvent (dodecane) was added onto the catalyst and kept overnight.

The reactor was flushed with argon (Ar, 99.999%) for 10 min followed by flushing with hydrogen for 5 min and pressurizing to 20 bar with hydrogen (AGA, 99.999%) at room temperature. Thereafter, the temperature was increased to the

desired one and the final pressure was adjusted to 30 bar total pressure. The reaction was commenced by starting the stirring. The external and internal mass transfer limitations were suppressed by using a high stirring speed (900 rpm) and small catalyst particles below 63 μm. The samples were taken from the reactor after certain time intervals and analyzed by GC. The gas sample was taken at the end of the reaction.

For vanillin HDO, the experiments were performed in an autoclave using 100 ml distilled water as a solvent. In a typical experiment vanillin initial concentration was 0.008 mol/l and 50 mg of the pre-reduced catalyst was used. The catalyst was covered with distilled water after reduction in Ar atmosphere prior to the experiment.

Gas chromatography for the liquid phase samples

Analysis of the samples in the HDO of guaiacol and isoeugenol was performed by a gas chromatograph using DB-1 capillary column (Agilent 122-103e) of 30 m length, 250 μm internal diameter and 0.5 μm film thickness was utilized for GC analysis. Helium (AGA, 99.996%) was applied as a carrier gas with flowrate of 1.7 ml/min. The temperature program for GC analysis is 60 °C (5 min)–3 °C/min–135 °C–15 °C/min-300 °C. The following external calibration standards for HDO of isoeugenol and guaiacol: isoeugenol (cis and trans) (Fluka, > 98%), guaiacol (Aldrich, ≥ 98%), dihydroeugenol (Sigma-Aldrich, ≥ 99%), cyclohexane (Lab Scan, 99%), heptane (Sigma-Aldrich, ≥ 99%), 2,5-dimethylhexane (Sigma-Aldrich, 99%), octane (Fluka, ≥ 99%), propylcyclohexane (Aldrich, 99%), 2-methoxycyclohexanone (TCI, > 95%), methoxycyclohexane (TCI, > 98%) were utilized for quantitative determination.

For the gas phase samples in the HDO of guaiacol, 1 ml of gas sample was taken from the reactor and analyzed with an Agilent 6890 N-GC equipped with HP-PLOTQ capillary column (30 m × 530 μm × 40 μm). The pressure and temperature were respectively 1.03 bar and 250 °C and the total gas flow was 55.2 ml/min (with the split ratio of 5:1). Detection was done by FID (300 °C) and TCD (250 °C). The mixtures of calibration gases from AGA contained carbon dioxide (1 V %), ethylene (0.099 V %), methane (1.02 V %), and methane (1 V %), ethane (1.03 V %), propane (0.981 V %), isobutene (0.983 V %), n-butane (0.96 V %) in helium.

Gas chromatography/mass spectrometry (Agilent Technologies 122-103e) was used to identify both gas and liquid phase compounds. DB-1 capillary column (Agilent 122-103e) of 30 m length, 250 μm internal diameter and 0.5μ. m film thickness was utilized for GC analysis. Helium (AGA, 99.996%) was applied as a carrier gas with the flowrate of 1.7 ml/min. The temperature program for separation of the liquid phase compounds was 60 °C (5 min)–3 °C/min–135 °C–15 °C/min–300 °C. The program applied for the gas phase samples was 40 or 60 °C (5 min) 3 °C/min–135 °C–15 °C/min–300 °C.

High performance liquid chromatography was applied for the analysis of samples obtained from HDO of vanillin. HPLC (Agilent Technologies 1100 Series) was supplied with a UV–vis photo diode array detector (273 nm) and a qternary pump. The utilized column was Ultra Techsphere ODS-5u (C18) (250 mm × 4.6 mm). The

non-stationary phase was a mixture of methanol and 0.5% phosphoric acid with the flowrate of 0.400 ml/min. The program set for the flow of the mixture (methanol + 0.5% phosphoric acid) using a gradient for the eluent given in Table S1. External calibration curves were made for vanillin and vanillyl alcohol.

Definitions

To assess the yield of the liquid phase products, gas chromatography based sum of the reactants and products in the liquid phase analysis (GCLPA) was calculated as follows:

$$GCLPA = \frac{GCLPA_t}{GCLPA_0} \times 100\%. \quad (1)$$

Here $GCLPA_0$ is the initial gas chromatography based sum of the reactants and products in the liquid phase analysis; $GCLPA_t$ is the gas chromatography based sum of the reactants and products in the liquid phase analysis at time t.

At a constant volume, conversion of the reactant was calculated in a conventional way using the following equation:

$$X_{a,t} = \frac{C_0 - C_i}{C_0} \times 100\%. \quad (2)$$

Here $X_{a,t}$ is the conversion of a particular reactant at time t, %; $C_{a,0}$ is the initial molar concentration of the reactant, mol/l; $C_{a,t}$ is the molar concentration of the reactant at time t, mol/l. The conversion of dihydroeugenol has been defined as its maximum concentration minus concentration of dihydroeugenol at time t divided by the maximum dihydroeugenol concentration, multiplied by 100%.

Results and discussion

Catalyst characterization results

The morphology of the catalysts was investigated by scanning electron microscopy and transmission electron microscopy. The SEM images (Fig. 2) did not show big differences in the shapes between fresh 3 wt% Ir/ZrO_2 and 10 wt% Ni/ZrO_2, except the size range. For Ir/ZrO_2 24 µm to 122 µm while for 10 wt% Ni/ZrO_2 this interval was somewhat larger (10-160 µm).

A possible metal leaching was excluded by comparing the mass ratio of Ir/Zr and Ni/Zr in the fresh and spent catalysts used in HDO of isoeugenol at 250 °C under 30 bar total pressure in hydrogen. For 3 wt% Ir/ZrO_2 and 10 wt% Ni/ZrO_2 no changes in the mass ratio of metal to Zr were observed by SEM–EDX. The Ir/Zr and Ni/Zr mass ratios were 0.1 and 0.2, respectively both in fresh and spent catalysts indicating no significant leaching in the spent catalysts.

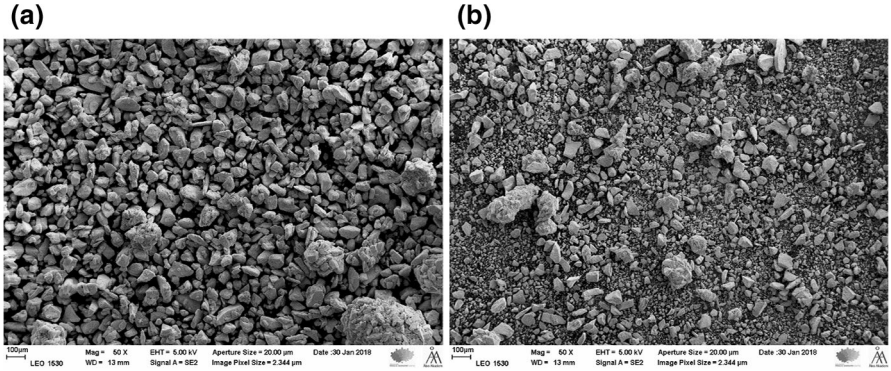

Fig. 2 SEM images for the fresh catalysts (magnification × 100). **a** Ir/ZrO_2, **b** 10 wt% Ni/ZrO_2

Based on 3 wt% Ir/ZrO_2 images, the particle size in the fresh and spent catalysts is 1.3 nm and 2.2 nm. From 10 wt% Ni/ZrO_2 catalyst images it was not possible to differentiate nickel and zirconia support.

TEM image for the reduced, fresh 10 wt% Ni/ZrO_2 contained large nickel nanoparticles are covered by nickel oxide thin layer and decorated by smaller nanocrystals of zirconia (Fig. 3a). Ni particle sizes varied in the range of 20 to 50 nm in diameter and separate nickel particles bigger than 100 nm could also be found. High iridium dispersion in the fresh 3 wt% Ir/ZrO_2 catalyst can be seen in the TEM image (Fig. 3b, Table 2). Although the spent catalyst exhibited also a high metal dispersion, some agglomerates were present, varying from 4 nm to 14 nm (Fig. 3c).

The specific surface area for the impregnated 10 wt% Ni/ZrO_2 used in the current work was 108 m^2/g while its pore volume was very low (Table 2). On the other hand, 3 wt% Ir/ZrO_2 catalyst contained a high pore volume in comparison with 10 wt% Ni/ZrO_2. According to Zhang et al. [15], 10 wt% Ni/ZrO_2 synthesized by deposition–precipitation had a specific surface area of only 6.2 m^2/g. According to [17], 5 wt% Ni/ZrO_2 prepared by incipient wetness impregnation had specific surface area of 130 m^2/g. Therefore, the catalysts made by impregnation method have larger specific surface area (> 100 m^2/g), while, deposition precipitation results in lower specific surface area.

Both 3 wt% Ir/ZrO_2 and 10 wt% Ni/ZrO_2 exhibit mainly weak Lewis acid sites (Table 3). In addition 10 wt% Ni/ZrO_2 exhibits also large amounts of Brønsted acidity, which is in accordance with literature [30] showing that the ratio of Brønsted to Lewis acidity determined by pyridine adsorption DRIFTs for 20 wt% Ni/ZrO_2 was 7.6 fold higher than for 20 wt% Ni/SiO_2. Brønsted acidity in 10 wt% Ni/ZrO_2 catalyst is originating from HNO_3 which was used to dissolve the Ni precursor and the pH of the precursor solution was between 1 and 2. After 2 h, NiO was formed on ZrO_2. It is known that Zr^{4+} present in ZrO_2 exhibits also Lewis acidity [31]. Furthermore, it is expected that part of Ni can be as Ni^{2+} on the surface of Ni/ZrO_2 since the concentration of Lewis acid sites was increasing 2.5 fold compared to that of Ir/ZrO_2. It is reasonable to suggest that a large amount of Ni is more difficult to reduce completely in comparison with Ir.

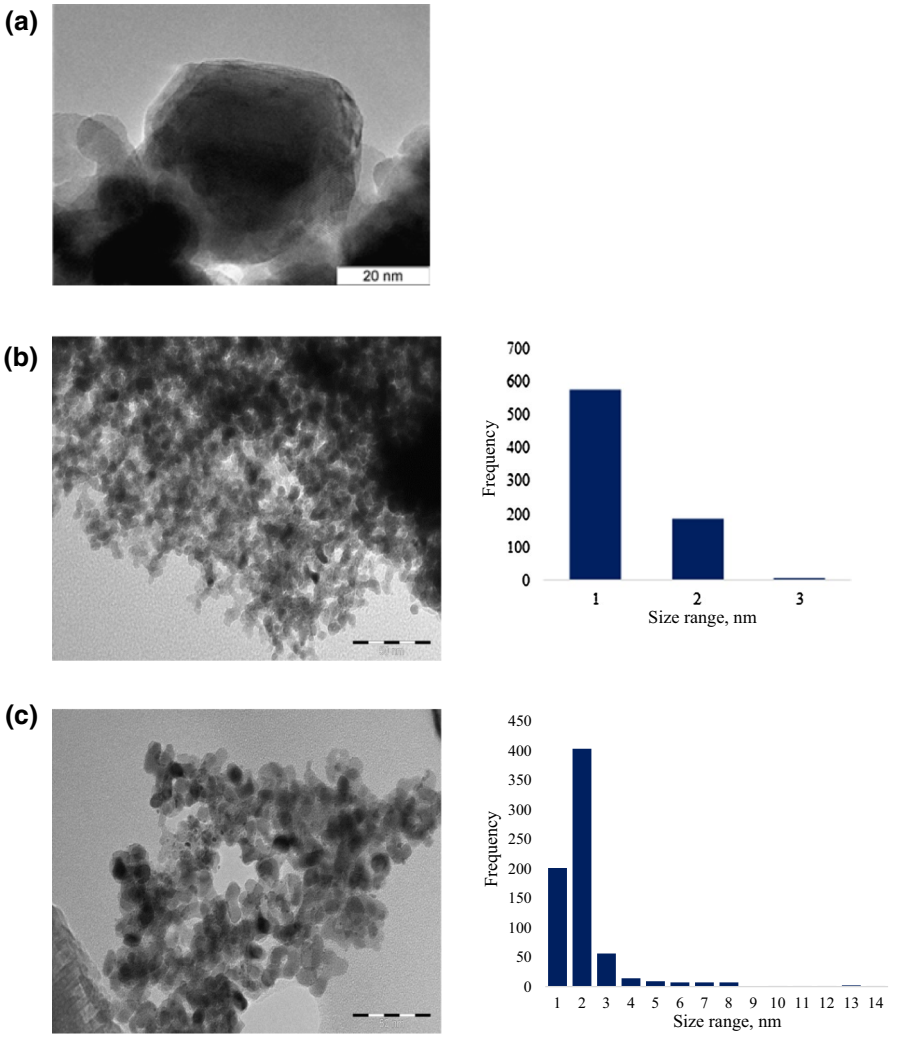

Fig. 3 TEM images and histograms of the metal particle sizes for **a** the fresh 10 wt% Ni/ZrO_2 and **b** fresh and **c** spent 3 wt% Ir/ZrO_2 catalyst used in isoeugenol HDO at 250 °C and 30 bar total pressure

Table 2 Catalyst characterization data

Catalyst	Specific surface area (m^2/g_{cat})	Pore volume (cm^3/g)	Calculated dispersion (%)	Metal particle size, TEM (nm)[a]
10 wt% Ni/ZrO_2	108	0.04	n.d.	1.1, 20–50[b]
3 wt% Ir/ZrO_2	91	0.24	77 (45)	1.3 (2.2)

[a]In parenthesis value for the spent catalyst

[b]Some particles also above 100 nm

Table 3 Brønsted and Lewis acid sites determined by FTIR

Catalyst	Brønsted acid sites (μmol/g_{cat})			Lewis acid sites (μmol/g_{cat})		
	250 °C	350 °C	450 °C	250 °C	350 °C	450 °C
3 wt% Ir–ZrO_2	1	0	0	157	0	0
10 wt% Ni–ZrO_2	70	0	0	398	1	0

Table 4 Organic coking results based on data via TGA

Catalyst	Organic coke in nitrogen, (%)
3 wt% Ir/ZrO_2	3.5[a]
10 wt% Ni/ZrO_2	2.9[a]
3 wt% Ir/ZrO_2	5.1[b]
10 wt% Ni/ZrO_2	3.2[b]

[a]Obtained using corresponding spent catalysts from isoeugenol HDO at 250 °C and 30 bar

[b]Obtained using corresponding spent catalysts from guaiacol HDO at 250 °C and 30 bar

TGA results for the fresh and spent catalysts in the guaiacol and isoeugenol HDO at 250 °C and 30 bar aluminum oxide and zirconium oxide supported catalysts) show that only small amounts of organic coke was obtained (Table 4), not being able to explain the low amounts of reactant and products analyzed by GC.

HDO results

Isoeugenol HDO

HDO of isoeugenol was investigated at 150 °C, 200 °C and 250 °C for 4 h both with 10 wt% Ni/ZrO_2 and 3 wt% Ir/ZrO_2 catalysts (Table 5, Figs. 4 and 5). The hydrogenation of isoeugenol to dihydroeugenol was very rapid already during heating as confirmed earlier [26, 32]. The transformation rate of isoeugenol after 1 min was, however very slow over Ni/ZrO_2 (Fig. 4a) indicating catalyst deactivation, which was confirmed by coking, since the spent catalyst contained carbon according to TGA results (Table 4). Conversion of dihydroeugenol over 10 wt% Ni/ZrO_2 increased with increasing temperature (Table 5). Complete conversion of isoeugenol was already achieved during heating the reactor at 250 °C. Dihydroeugenol was, however, transformed quite slowly over Ni/ZrO_2 catalysts, about 0.004 mol/$ming_{Ni}$ during 1 to 30 min.

Isoeugenol was converted over Ir/ZrO_2 already at 150 °C 82% after 1 min reaction time and for the two other temperatures, 200 °C and 250 °C it was converted even faster and complete conversion of isoeugenol was obtained at all temperatures (Table 5). Dihydroeugenol conversion increased with increasing temperature

Table 5 Results from HDO of isoeugenol over Ni/ZrO_2 and Ir/ZrO_2 catalysts under the total pressure of 30 bar in dodecane

Catalyst	Temperature (°C)	Conversion of IE (DH) after 240 min (%)[a]	Sum of masses of reactant and products in liquid phase analyzed by GC (%)	Yield of dihydroeugenol (%) after 240 min	Yield of propylcyclohexane (%) after 240 min	Yield of trimethylbenzene (%) after 240 min
10 wt% Ni/ZrO_2	150	100 (5)	99	91	0	12
	200	100 (81)	19	17	1	0
	250	100 (95)	15	3	16	0
3 wt% Ir/ZrO_2	150	100 (17)	69	69	2	0
	200	100 (34)	56	52	4	0
	250	100 (0)	37	0	33	4

[a]In parenthesis conversion of dihydroeugenol (DH)

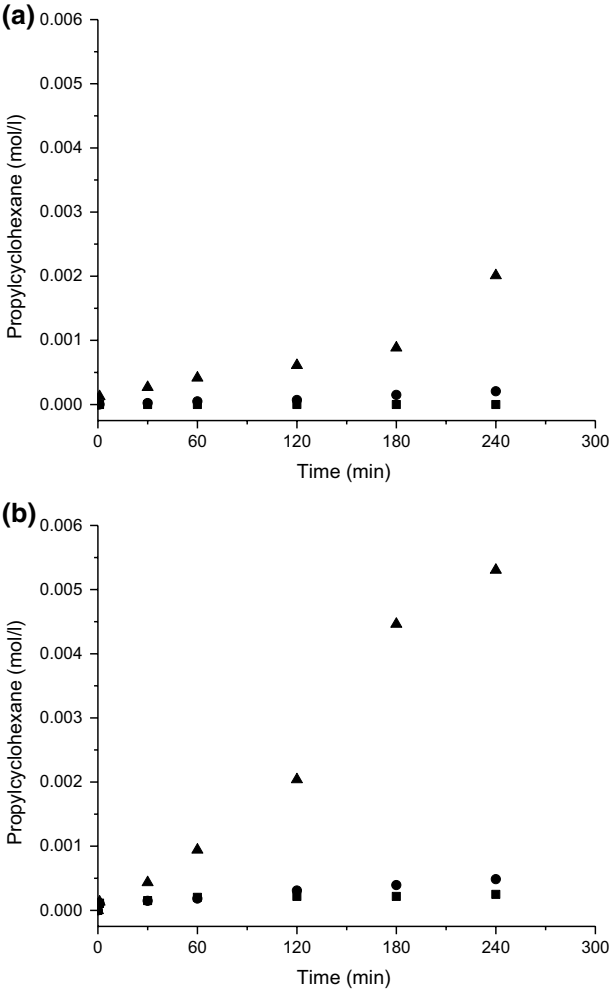

Fig. 4 Kinetics for formation of propylcyclohexane in HDO of isoeugenol over **a** 10 wt% $NiZrO_2$ and **b** 3 wt% Ir/ZrO_2 catalysts. Notation (filled square) 150 °C, (filled circle) 200 °C and (filled triangle) 250 °C

(Table 5), but the initial transformation rate of dihydroeugenol was, however, rather slow at 250 °C being 0.002 mol/min/g_{Ir} and even after 240 min at 250 °C not complete conversion of dihydroeugenol was obtained (Table 5). It can be concluded that dihydroeugenol transformed initially 1.8-fold faster over Ni/ZrO_2 compared to Ir/ZrO_2. This can be related to hydrogenolysis activity of Ir [19] and smaller particle sizes being more prone to deactivation in comparison with Ni.

The GCLPA decreased over both Ni/ZrO_2 and Ir/ZrO_2 catalysts with increasing reaction temperature and increasing conversion being the lowest for Ni/ZrO_2 at 250 °C (Table 5). The reason for such lower GCLPA obtained by Ni/ZrO2 is its high activity for formation of gaseous products. Furthermore, Ir/ZrO_2 in

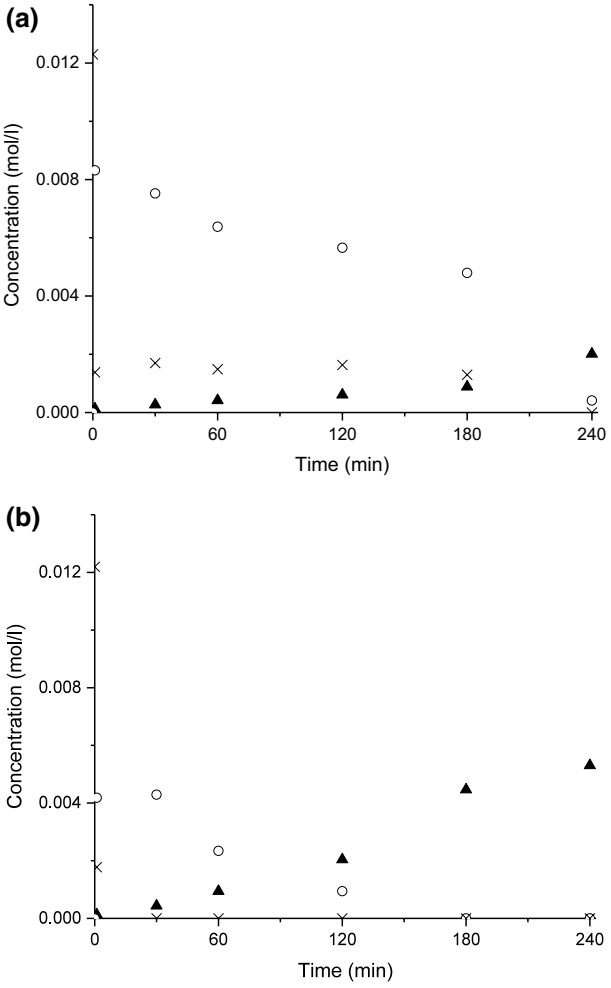

Fig. 5 Kinetics in HDO of isoeugenol over **a** $NiZrO_2$ and **b** Ir/ZrO_2 catalysts. Conditions: 250 °C, total pressure 30 bar, initial isoeugenol concentration 0.012 mol/l, solvent dodecane, catalyst mass 50 mg. Notation: isoeugenol (multiplication sign), dihydroeugenol (open circle) and propylcyclohexane (filled triangle)

the current work exhibited only Lewis acidity, whereas Ni/ZrO_2 contained also weak Brønsted acid sites (Table 3). As a comparison Pt supported Beta zeolites containing both Brønsted and Lewis acid sites gave in isoeugenol HDO [7] the GCLPA of 45-61% at 200 °C under 30 bar hydrogen. It can be thus concluded that GCLPA with Ir and Ni supported on ZrO_2 was about the same as for Pt–H-Beta catalysts. This comparison indicates that both metal and support selection is very important for obtaining high GCLPAs. Ir is known to be very active in hydrogenolysis [20], while Ni facilitates methanation. Furthermore, the mass balance closure in HDO of isoeugenol using $Ir–Re/Al_2O_3$ was 79% under comparative

conditions showing clearly that the selection of support and the amount of iridium are crucial for mass balance closure [26]. The low GCLPA values with the catalysts from this work is due to formation gaseous products [26]. Furthermore, oligomer product formation from isoeugenol in HDO of the latter using Ir–Re/Al_2O_3 catalysts has been previously confirmed via performing extraction of the spent catalyst with heptane and analyzing the extract phase by SEC [26]. Thus the most plausible reasons for a low mass balance closure are formation of oligomers and gaseous products. The results for Ir/ZrO_2 can be also partially explained by large amounts of alkanes such as hexane, heptane and octane formed in the presence of only the solvent, dodecane with Ir/ZrO_2 at 250 °C and 30 bar total pressure. These compounds have not been taken into account during GCLPA calculations when using isoeugenol as a reactant, because otherwise it leads to GCLPA higher than 100% in the current experimental setup and it would be impossible to separate formation of alkanes from the solvent and from the reactant. In comparison with literature the mass balance closure in HDO of 4-propylphenol over different Pt supported catalysts under 40 bar hydrogen at 200 °C in water was 78% at complete conversion over Pt/ZrO_2, whereas the comparative value with Pt/C was 98% [25] indicating also that zirconia support has a negative effect on the mass balance closure. On the other hand, this result cannot be generalized since reaction conditions, such as high hydrogen pressure, increases the carbon mass balance, as was the case with phenol HDO giving 90% total mass balance closure under 100 bar at 275 °C [10].

The yield of the deoxygenated product, propylcyclohexane increased, as expected with increasing temperature for both ZrO_2 supported catalysts. It is also interesting to note that only a minor increase in formation rates of propylcyclohexane over Ir/ZrO_2 was observed when increasing the reaction temperature from 150 °C to 200 °C, whereas at 250 °C the initial formation rate of propylcyclohexane was 2.9 fold that at 200 °C (Fig. 4). The initial formation rate for propylcyclohexane over Ni/ZrO_2 at 250 °C was 11-fold that calculated at 200 °C indicating that Ni/ZrO_2 requires higher temperature for HDO than Ir/ZrO_2. The highest yields for propylcyclohexane were obtained at 250 °C being 16% and 33% for Ni/ZrO_2 and Ir/ZrO_2, respectively, were obtained. These yields are much lower compared to those obtained over Pt–H-Beta-300 and Pt–H-Beta-150 (the number in the catalyst name denotes SiO_2/Al_2O_3 ratio) being at 200 °C 74% and 64% [7] and those reported by Zhang et al. [15]. In [15], 98% selectivity of propylcyclohexane was obtained at 300 °C under 50 bar hydrogen in 8 h using a mixture of eugenol, vanillin, guaiacol, phenol and trans-anethole as a feedstock. In [15] both hydrogen pressure and reaction temperature were much higher than in the current case, most probably enhancing activity of Ni/ZrO_2. Noteworthy is also that formation of 1,2,4-trimethylbenzene was observed over 10 wt% Ni/ZrO_2 at 150 °C (Table 5) indicating that despite demethoxylation of the formed dihydroeugenol, hydrogenation of the phenyl ring was, however, not very efficient under these conditions. In addition C–C bond breaking in the propyl chain occurred. This result is interesting since e.g. hydrogenation of propylbenzene is thermodynamically feasible at 200 °C under 30 bar hydrogen [7], but not at 300 °C under 30 bar.

Guaiacol HDO

In the hydrodeoxygenation of guaiacol over 10 wt% Ni/ZrO_2 at 250 °C and 30 bar total pressure the initial guaiacol transformation rate between 1 and 30 min was 1.6 mmol/min g_{Ni} and complete conversion of guaiacol was obtained after 240 min (Fig. 5a). GCLPA is rather low being 54% for 10 wt% Ni/ZrO_2 (Table 6). To complete the GCLPA, both organic coke and gas phase analysis were performed. Using thermogravimetric analysis, organic coke was estimated from the temperature ramp between 100 and 1000 °C, i.e. excluding water content for both catalysts. GCLPAs increased to 48 and 57% for 3 wt% Ir/ZrO_2 and 10 wt% Ni/ZrO_2, correspondingly, showing that this solid fraction could only slightly increase the GCLPA levels. Thus gas samples were taken after 4 h of the reaction and analyzed by GC–MS after 4 h of reaction. Methane was present in the gas phase together with ethane (Table S2, Fig. S3). Methanation is expected to occur via hydrogenation of CO which is thermodynamically feasible already at 227 °C at which the Gibbs free energy for methanation is -96.4 kJ/mol [33]. In addition it is known that Ni is promoting methanation.

Over Ir/ZrO_2 catalyst the initial transformation rate of guaiaocl was 2.1 mmol/mingIr being higher than that for Ni/ZrO_2 and complete conversion of guaiacol was obtained in 4 h (Table 6). The GCLPA for Ir/ZrO_2 was lower than for Ni/ZrO_2 (Table 6) due to the high hydrogenolysis activity of Ir, as stated above, promoting formation of gaseous products. When comparing the gas phase analysis results (Fig. S3) of Ir/ZrO_2 and Ni/ZrO_2 by GC–MS it can be observed that the distribution of gases for Ir/ZrO_2 catalyst is broader in comparison with 10 wt% Ni/ZrO_2. Over Ir/ZrO_2 catalyst CH_4 gas was produced more than over 10 wt% Ni/ZrO_2 (retention time of 1.1 min in Fig. S3). In demethoxylation, the formed alkoxide group can be adsorbed on the metal surface and hydrogenated to form methane and water. Ethane gave the highest peak at the retention time of 1.2 min for both catalysts (Fig. S3). Formation of more gaseous products over 3 wt% Ir/ZrO_2 than over 10 wt% Ni/ZrO_2 could explain lower GCLPA (43% vs. 54%).

The main product in guaiacol HDO over 10 wt% Ni/ZrO_2 at 250 °C under 30 bar total pressure was cyclohexanol showing that this catalyst was active in hydrogenation of phenyl ring, but at the same time exhibiting lower HDO activity. In addition, large amounts of 2-methoxycyclohexanone were initially formed. The ratio between the formed cyclohexanol to 2-methoxycyclohexanone at 1 min reaction time was 1.8 indicating that Ni/ZrO_2 catalyst was initially very active in hydrogenation of the phenyl ring and in demethoxylation. 2-methoxycyclohexanone can be formed either via isomerization of 2-methoxycyclohexenol to corresponding ketone or from guaiacol. This result is in accordance with thermodynamics, since it is known that dissociation of methoxy bond requires less energy (343 kJ/mol) compared to dissociation of an alcohol group (385 kJ/mol) [34]. Ni/ZrO_2 was, however, able to only partially transform 2-methoxycyclohexanonone to cyclohexane (Fig. 5a) and the yield of fully deoxygenated product, cyclohexane was very low, being only 2% (Table 6). It can be seen from the kinetic plot that 2-methoxycyclohexanone did not react further since its concentration remained constant. Furthermore cyclohexanol concentration increased during 4 h reaction, indicating that 10 wt% Ni/ZrO_2 catalyst mainly containing weak Lewis acid sites (Table 3) was not active in hydrodeoxygenation to

Table 6 Results from HDO of guaiacol and vanillin over Ni/ZrO_2 and Ir/ZrO_2 catalysts under the total pressure of 30 bar in dodecane. Conditions: Guaiacol HDO at 250 °C in dodecane as a solvent and vanillin HDO at 100 °C in distilled water. The initial concentrations of guaicol and vanillin are 0.016 mol/l and 0.007 mol/l, respectively

catalyst	Conversion of guaiacol after 240 min (%)	Sum of the masses of reactant and products in liquid phase analyzed by GC (%)	Yield of the sum of 2-methoxycyclohexanone and 2-methoxycyclohexanol (%) after 240 min	Yield of methoxycyclohexane (%) after 240 min	Yield of cyclohexanol (%) after 240 min	Yield of cyclohexane (%) after 240 min
10 wt% Ni/ZrO_2	100	54	23	0	36	2
3 wt% Ir/ZrO_2	100	43	9	1	29	14

	Conversion of vanillin after 240 min (%)	Sum of the masses of reactant and products in liquid phase analyzed by GC (%)	Yield of vanillyl alcohol (%)
10 wt% Ni/ZrO_2	95	92	86
3 wt% Ir/ZrO_2	100	78	77

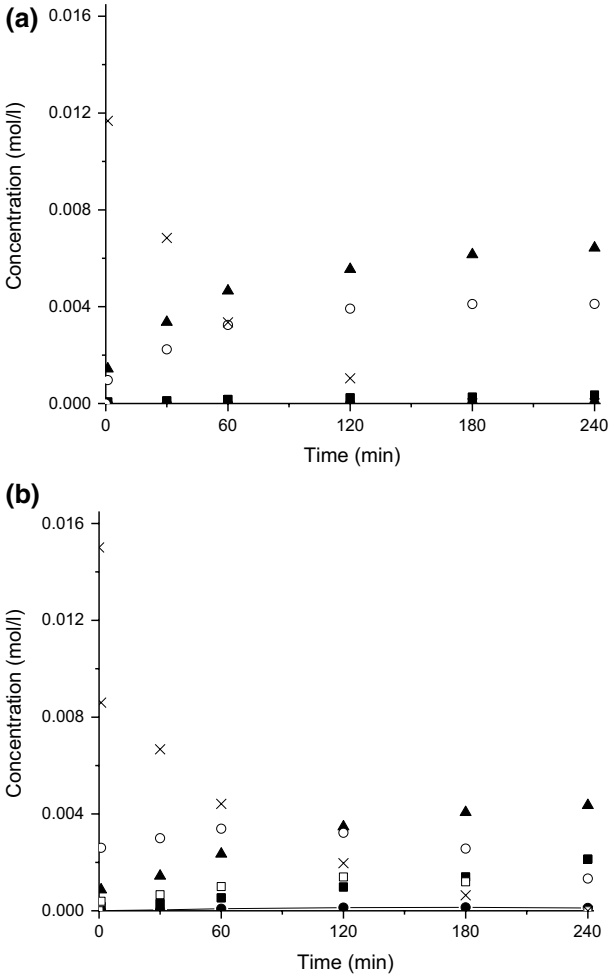

Fig. 6 Kinetics in HDO of guaiacol over **a** Ni/ZrO_2 and **b** Ir/ZrO_2 catalysts. Conditions: 250 °C, total pressure 30 bar, initial guaiacol concentration 0.016 mol/l, solvent dodecane, catalyst mass 50 mg. Notation: guaiacol (multiplication sign), methoxycyclohexane (filled circle), 2-methoxy-cyclohexanone (open circle), 2-methoxycyclohexanol (open square), cyclohexanol (filled triangle) and cyclohexane (filled square)

cyclohexane. As comparison with the literature [10], 5 wt% Ni/ZrO_2 was reported to be very efficient in hydrodeoxygenation of phenol at 275 °C under 100 bar yielding 80 mol % of cyclohexane and 10 mol % cyclohexanol. Furthermore, high selectivity towards cyclohexane, 75% was obtained over Ni/ZrO_2 at 43% conversion [15]. The conditions in their work [14] were, however, very much more severe compared to the current work.

The main product in guaiacol HDO over 3 wt% Ir/ZrO_2 was also cyclohexanol (Table 6). Initially 2-methoxycyclohexanone was the main product and its concentration started to decrease after 120 min reaction time (Fig. 6b). The second major

product already in the beginning of the reaction was cyclohexanol and its concentration increased during 4 h reaction time. This compound reacted further to cyclohexane, and its concentration was increasing during the reaction. The initial ratio between the yield of cyclohexanol to 2-methoxycyclohexanone was 0.4 showing that Ni/ZrO_2 was initially 4.5-fold more active in transforming 2-methoxycyclohexanone to cyclohexanol than Ir/ZrO_2. After prolonged time Ir/ZrO_2 was able to transform 2-methoxycyclohexanone to cyclohexanol and also substantial yield of cyclohexane (14% yield) was formed (Fig. 6b, Table 6). This intermediate, 2-methoxycyclohexanonone was, however, only partially transformed to cyclohexane (Fig. 6b).

As a conclusion it can be stated that Ir/ZrO_2 was more active than Ni/ZrO_2 to produce fully deoxygenation product cyclohexane. The drawback with this catalyst was the low liquid phase mass balance closure due to high hydrogenolysis activity of Ir forming also large amounts of the gaseous products.

Vanillin HDO

Hydrodeoxygenation of vanillin was performed using 10 wt% Ni/ZrO_2 and 3 wt% Ir/ZrO_2 at 100 °C and 30 bar total pressure in the presence of hydrogen and water used as a solvent (Fig. 7). Vanillin concentration decreased during the initial heating probably due to strong adsorption of it on the catalyst surface similar to observations of Santos et al. [5]. Initially the transformation rate of vanillin between 1 and 30 min of the reaction time was 0.0035 mol/min/g_{Ni} for Ni/ZrO_2 being almost the same whereas for Ir/ZrO_2 it was (0.003 mol/min/g_{Ir}). Both of these catalysts exhibited Ni particles of rather small sizes (Table 2) and the differences in their performance were minor. The catalytic activity in vanillin transformation was, however, retarded substantially over Ni/ZrO_2 after 60 min, whereas Ir/ZrO_2 was more active. The former catalyst has more Lewis acid sites and also small amounts of Bronsted acid sites (Table 3), which can cause catalyst deactivation. Vanillin conversions were nearly the same for 10 wt% Ni/ZrO_2 and Ir/ZrO_2 being 94% and 99%, respectively after 4 h. GCLPA was the best over 10 wt% Ni/ZrO_2 being 92%. Over Ir/ZrO_2 the GCLPA was 78% indicating higher hydrogenolysis activity of Ir [20].

Using 10 wt% Ni/ZrO_2 catalyst, the main product was vanillin alcohol with the yield of 86% after four hours of the reaction unconverted vanillin was also present (Table 6, Fig. 7a). No other products were seen in HPLC, such as p-cresol or *p*-creosol, due to low activity (mild acidity) in hydrodeoxygenation. Analogously to nickel the main product over Ir/ZrO_2 was also vanillyl alcohol with the yield of 77% (Table 6, Fig. 7b). It can be concluded that these catalysts did not facilitate deoxygenation of vanillin under the studied reaction conditions. Vanillin HDO requires much more severe conditions. In particular experiments at 300 °C under 50 bar of hydrogen utilization of $Ni/SiO_2–ZrO_2$ gave at 83% conversion 65% selectivity to methylcyclohexane [4]. Typically, partial deoxygenation of vanillin in water as a solvent was obtained forming *p*-creosol as the main product under 30 bar at 100 °C over Pd/C [5]. This comparison shows that Pd has electronic properties facilitating formation of *p*-creosol under mild conditions, whereas Ni as a transition metal is less active.

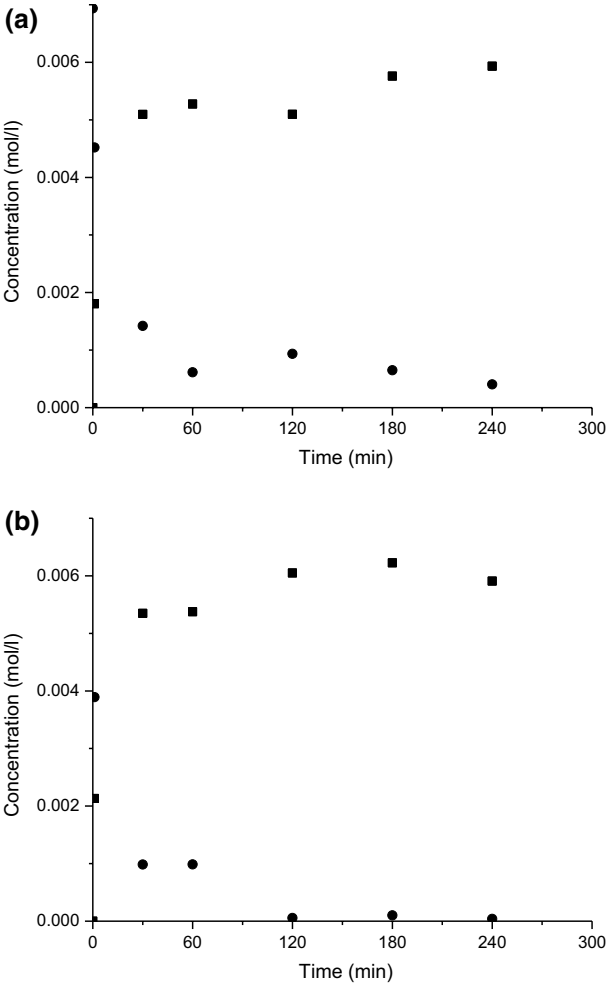

Fig. 7 Kinetics in HDO of vanillin over **a** $NiZrO_2$ and **b** Ir/ZrO_2 catalysts. Conditions: 250 °C, total pressure 30 bar, initial vanillin concentration 0.008 mol/l, solvent water, catalyst mass 50 mg. Notation: vanillin (filled circle) and vanillyl alcohol (filled square)

Conclusions

A comparative investigation of isoeugenol, guaiacol and vanillin hydrodeoxygenation was performed using Ni and Ir supported ZrO_2 catalysts prepared by the incipient wetness method. Both catalysts exhibited Lewis acidity, whereas Ni/ZrO_2 contained also weak Brønsted acid sites.

The deoxygenation efficiency of Ni/ZrO_2 was low in isoeugenol transformation at 150 °C under 30 bar, increasing with temperature elevation. Analogous results were found for Ir/ZrO_2. The drawback with these catalysts in isoeugenol transformation was the low liquid phase mass balance closure due to formation of large amounts

of gas phase products in the liquid phase. In guaiacol HDO over 3 wt% Ir/ZrO_2, the maximum yield of cyclohexane at 250 °C under 30 bar is 14%. The main product was cyclohexanol indicating that this catalyst facilitated only partial deoxygenation, which can be related to low acidity. Ni/ZrO_2 also gave cyclohexanol as the main product.

Vanillin transformation in water at 100 °C under 30 bar resulted in formation of vanillyl alcohol as the main product indicating that Ir and Ni supported ZrO_2 catalysts at these conditions provide only partial HDO of vanillin.

Acknowledgements Open access funding provided by Abo Akademi University (ABO). The authors acknowledge the financial support provided by Neste Corporation.

References

1. Mäki-Arvela P, Murzin DYu (2017) Hydrodeoxygenation of lignin-derived phenols: from fundamental studies towards industrial applications. Catalysts 7(9):1–40
2. Boscagli C, Raffelt K, Zevaco TA, Olbrich W, Otto TN, Sauer J, Grundwaldt JD (2015) Mild hydrotreatment of the light fraction of fast-pyrolysis oil produced from straw over nickel-based catalysts. Biomass Bioenergy 83:525–538
3. Oh S, Choi HS, Choi IG, Choi JW (2017) Evaluation of hydrodeoxygenation reactivity of pyrolysis bio-oil with various Ni-based catalysts for improvement of fuel properties. RSC Adv 7:15116–15126
4. Zhang X, Tang W, Zhang Q, Wang T, Ma L (2017) Hydrocarbons production from lignin-derived phenolic compounds over Ni/SiO_2 catalyst. Energy Proc 105:518–523
5. Santos JL, Alda-Onggar M, Fedorov V, Peurla M, Eränen K, Mäki-Arvela P, Centeno MÁ, Murzin DYu (2018) Hydrodeoxygenation of vanillin over carbon supported metal catalysts. Appl Catal A 561:137–149
6. He L, Qin Y, Lou H, Chen P (2015) Highly dispersed molybdenum carbide nanoparticles supported on activated carbon as an efficient catalyst for the hydrodeoxygenation of vanillin. RSC Adv 5:43141–43147
7. Bomont L, Alda-Onggar M, Fedorov V, Aho A, Peltonen J, Eränen K, Peurla M, Kumar N, Wärnå J, Russo V, Mäki-Arvela P, Grenman H, Lindblad M, Murzin DYu (2018) Production of cycloalkanes in hydrodeoxygenation of isoeugenol over Pt- and Ir- modified bifunctional catalysts. Eur J Inorg Chem 24:2841–2854
8. Gonzales C, Marin P, Diaz FV, Ordonez S (2016) Gas-phase hydrodeoxygenation of benzaldehyde, benzyl alcohol, phenyl acetate and anisole over precious metal catalysts. Ind Eng Chem Res 55:2319–2327
9. Teles CA, Rabelo-Neto RC, Jacobs G, Davis BH (2017) Resasco DE, Noronha FB, Hydrodeoxygenation of phenol over zirconia-supported catalysts: the effect of metal type on reaction mechanism and catalyst deactivation. ChemCatChem 9:2850–2863
10. Mortensen PM, Grunwaldt JD, Jensen PA, Jensen AD (2013) Screening of catalysts for hydrodeoxygenation of phenol as a model compounds for bio-oil. ACS Catal 3:1774–1785
11. Chen CJ, Bhan A (2017) Mo_2C modification by CO_2, H_2O, and O_2: effect of oxygen content and oxygen source on rates and selectivity of m-cresol hydrodeoxygenation. ACS Catal 7:1113–1122
12. Sulman A, Mäki-Arvela P, Bomont L, Fedorov V, Alda-Onggar M, Smeds A, Hemming J, Russo V, Wärnå J, Käldström M, Murzin DYu (2018) Vanillin hydrodeoxygenation: kinetic modelling and solvent effect. Catal Lett 148:2856–2868

13. Goncalves VOO, de Souza PM, Cabioc'h T, da Silva VT, Noronha FB, Richard F (2017) Hydrodeoxygenation of m-cresol over nickel and nickel phosphide based catalysts. Influence of the nature of the active phase and the support. Appl Catal B 219:619–628
14. Liu X, Jia W, Xu G, Zhang Y, Fu Y (2017) Selective hydrodeoxygenaiton of lignin-derived phenols to cyclohexanols over Co-based catalsyts. ACS Sust Chem Eng 5:8594–8601
15. Zhang X, Zhang Q, Wang T, Ma L, Yu Y, Chen L (2013) Hydrodeoxygenation of lignin-derived phenolic compounds to hydrocarbons over Ni/SiO_2–ZrO_2 catalysts. Biores Technol 134:73–80
16. Lee CR, Yoon JS, Suh YW, Choi JW, Ha JM, Suh DJ, Park YK (2012) Catalytic roles of metals and supports on hydrodeoxygenation of lignin monomer guaiacol. Catal Commun 17:54–58
17. Mortensen PM, Gardini D, de Carvalho HWP, Damsgaard CD, Grunwaldt JD, Jensen PA, Wagner JK, Jensen AD (2014) Stability and resistance of nickel catalysts for hydrodeoxygenation: carbon deposition and effects of sulfur, potassium, and chlorine in the feed. Catal Sci Technol 4:3672–3686
18. Lu M, Du H, Wei B, Zhu J, Li M, Shan Y, Shen J, Song C (2017) Hydrodeoxygenation of guaiacol on Ru catalysts: influence of TiO_2–ZrO_2 composite oxide supports. Ind Eng Chem Res 56:12070–12079
19. Gutierrez A, Kaila RK, Honkela ML, Slioor R, Krause AOI (2009) Hydrodeoxygenation of guaiacol on noble metal catalysts. Catal Today 147(3–4):239–246
20. Chen K, Mori K, Watanabe H, Nakagawa Y, Tomishige K (2012) C–O bond hydrogenolysis of cyclic ethers with OH groups over rhenium-modified supported iridium catalysts. J Catal 294:171–183
21. Sullivan RJ, Latifi E, Chung BKM, Soldatov DV, Schlaf M (2014) Hydrodeoxygenation of 2,5-hexanedione and 2,5-dimethylfuran by water, air and acid-stable homogeneous ruthenium and iridium catalysts. ACS Catal 4:4116–4128
22. Bykova MV, Zavarukhin SG, Trusov LI, Yakovlev VA (2013) Guaiacol hydrodeoxygenation kinetics with catalyst deactivation taken into consideration. Kinet Catal 54:40–48
23. Roldugina EA, Naranov ERE, Maximov AL, Karakhanov EA (2018) Hydrodeoxygenation of guaiacol as a model compoubnd of bio-oil in methanol over mesoporous noble metal catalysts. Appl Catal A. https://doi.org/10.1016/j.apcata.2018.01.2018
24. Liu S, Dutta S, Zheng W, Gould NS, Cheng Z, Xu B, Saha B, Vlachos DG (2017) Catalytic hydrodeoxygenation of high carbon furylmethanes to renewable jet-fuel ranged alkanes over a rhenium-modified iridium catalyst. ChemSusChem 10:3225–3234
25. Ohta H, Kobayashi H, Hara K, Fukuoka A (2011) Hydrodeoxygenation of phenols as lignin models under acid-free conditions with carbon-supported platinum catalysts. ChemComm 47:12209–12211
26. Alda-Onggar M, Mäki-Arvela P, Eränen K, Aho A, Hemming J, Paturi P, Peurla M, Lindblad M, Simakova IL, Murzin DYu (2018) Hydrodeoxygenation of isoeugenolover alumina supported Ir-, Pt- and Re catalysts. ASC Sust. Chem. Eng. https://doi.org/10.1021/acssuschemeng.8b03035
27. Santillan-Jiminez E, Perdu M, Pace R, Morgan T, Crocker M (2015) Activated carbon, carbon nanofiber and carbon nanotube supported molybdenum carbide catalysts for the hydrodeoxygenation of guaiacol. Catalyst 5:424–441
28. Nabgan W, Abdullah TAT, Mat R, Nabgan B, Gambo Y, Johari A (2016) Evaluation of reaction parameters of the phenol steam reforming over Ni/Co on ZrO_2 using the full factorial experimental design. Appl Sci 6(223):1–21
29. Emeis CA (1993) Determination of integrated molar extinction coefficients for infrared absorption bands of pyridine adsorbed on solid acid catalysts. J Catal 141:335–347
30. Kumar VV, Naresh G, Sudhakar M, Anjaneyulu C, Bhargava SK, Tardio J, Reddy VK, Padmasri AH, Venugopal A (2016) An investigation on the influence of support type for Ni catalyzed vapour phase hydrogenation of aqueous levulinic acid to γ-valerolactone. RSC Adv 6:9872–9879
31. Rabee AIM, Mekhemer GAH, Osatiashtiani A, Isaacs MA, Lee AF, Wilson K, Zaki MI (2017) Acidity-reactivity relationships in catalytic esterification over ammonium sulfate-derived sulfated zirconia. Catalysts 7(204):1–16
32. Bjelić A, Grilc M, Likozar B (2018) Catalytic hydrogenation and hydrodeoxygenation of lignin-derived model compound eugenol over Ru/C: intrinsic microkinetics and transport phenomena. Chem Eng J 333:240–259
33. Barin I (1989) Thermochemical data of pure substances. VCH, Weinheim
34. Benzon SW (1968) Thermochemical kinetics: methods for estimation of thermochemical data rate parameters. John Wiley & Sons, Inc., New York